



Fermi National Accelerator Laboratory

FERMILAB-Pub-83/52-EXP
7190.497

(Submitted to Phys. Rev. Lett.)

A PRECISE MEASUREMENT OF THE Σ^+ MAGNETIC MOMENT

C. Ankenbrandt, J. P. Berge, A. E. Brenner, J. Butler, K. Doroba,
J. E. Elias, J. Lach, P. Laurikainen, J. MacLachlan, and J. Marriner
Fermi National Accelerator Laboratory, Batavia, Illinois 60510

and

E. McCliment
Department of Physics, University of Iowa, Iowa City, Iowa 52242

and

E. W. Anderson and A. Breakstone
Department of Physics, Iowa State University, Ames, Iowa 50011

and

T. Cardello, P. S. Cooper, L. J. Teig, J. L. Thron, and Y. W. Wah
J. W. Gibbs Laboratory, Yale University, New Haven, Connecticut 06511

June 1983



A PRECISE MEASUREMENT OF THE Σ^+ MAGNETIC MOMENT

C. Ankenbrandt, J.P. Berge, A.E. Brenner, J. Butler, K. Doroba (a)
J.E. Elias, J. Lach, P. Laurikainen (b), J. MacLachlan, and J. Marriner

Fermi National Accelerator Laboratory, Batavia, Illinois 60510

E. McCliment

Department of Physics, University of Iowa, Iowa City, Iowa 52242

E.W. Anderson and A. Breakstone

Department of Physics, Iowa State University, Ames, Iowa 50011

T. Cardello, P.S. Cooper, L.J. Teig, J.L. Thron, and Y.W. Wah

J. W. Gibbs Laboratory, Yale University,
New Haven, Connecticut 06511

June, 1983

ABSTRACT

The Σ^+ magnetic moment is measured to be 2.38 ± 0.02 nuclear magnetons using a sample of 44457 polarized $\Sigma^+ \rightarrow p\pi^0$ decays in a charged hyperon beam. The inclusively produced Σ^+ in this 212 GeV/c beam have a polarization of about 0.20 for production angles between 2.5 and 7.0 mrad. Their direction of polarization is opposite to that of Λ^0 produced in a comparable kinematic region.

The magnetic moments of the baryons have long been considered of fundamental importance and a powerful tool for studying the internal structure of the baryons¹. High energy polarized hyperon beams have recently become available, making possible precise measurements of the hyperon magnetic moments². Before these recent experiments were performed, the data could be adequately described by a SU(6) quark model³. These more precise experiments show systematic discrepancies from the SU(6) model; there is no convincing quantitative theory⁴. More recently, crude calculations of some baryon magnetic moments have been made with QCD using lattice gauge theory techniques⁵. This paper reports a new precision measurement of the Σ^+ magnetic moment.

In the experimental setup shown in Fig. 1, a 400 GeV/c proton beam was incident on a 1 interaction length copper target at an angle with respect to the horizontal plane. This angle could be varied between -7 and 7 mrad. The target was placed at the upstream end of a 7m long magnet having a field integral of 14.4 Tm. The y axis is defined to be vertical and the z axis to be in the direction of the secondary Σ^+ beam momentum. With these definitions, the polarization at the target was parallel (or anti-parallel) to the x axis. The polarization precessed about the vertical magnetic field through an angle ξ in the x-z plane proportional to the anomalous magnetic moment of the Σ^+ , given by

$$\xi = \frac{1}{2} \cdot (g-2) \cdot \langle \eta \rangle \cdot \theta_B \quad (1)$$

Where $\langle \eta \rangle = \langle P \rangle / m_{\Sigma^+}$, $\langle P \rangle$ is the momentum of the central trajectory which is proportional to the magnetic field integral

in the magnet, and θ_B is the bend angle in the magnet. The magnetic moment, μ_Σ , of the Σ^+ is related to g by

$$\mu_\Sigma = \frac{gm_p}{2m_\Sigma} \mu_N \quad (2)$$

where m_p (m_Σ) is the proton (Σ^+) mass and $\mu_N = e\hbar/2m_p c$ is the nuclear magneton.

The 210 GeV/c secondary beam emerging from the magnet was limited by a tungsten channel to an emittance of ± 16 GeV/c and 1 μ sr. The beam typically contained 50,000 particles in a 1 second pulse. The Σ^+ constituted 0.5% of the emerging beam; about half of them decayed in the region of the high resolution proportional chambers (PWC) shown in Fig. 1.

The $\Sigma^+ \rightarrow p\pi^0$ trigger consisted of the coincidence of a single beam track defined by scintillation counters in the PWC region, a downstream counter to detect the energetic proton, and a total energy deposition in the lead glass of > 1 GeV. The trigger rate was about 100/pulse. About 1/3 of the triggers were genuine Σ^+ events; the remainder were background from interactions in the PWCs and drift chambers. Other triggers were used to provide calibration data. These included a beam trigger which required the beam scintillation counters only, and a $\Sigma^+ \rightarrow n\pi^+$ trigger which required, in addition, a neutral particle signal from the neutron calorimeter.

The Σ^+ particles which decayed downstream of the PWC region were measured to an accuracy (σ) of about 1.5 GeV/c in momentum, 50 μ rad in azimuth and 30 μ rad in dip. Protons from the decay

$\Sigma^+ \rightarrow p\pi^0$ emerging from the 20 m decay region were measured with an accuracy of $\Delta p/p=1\%$, 60 μrad in azimuth and 40 μrad in dip.

The analysis was performed with events where a beam track was found in the PWCs and a decay track was found in the drift chambers. The beam track was required to extrapolate in the vertical view back to the center of the 2 mm high target to within ± 3 mm. The decay track was required to be properly reconstructed using the most downstream drift chamber in order to obtain the best resolution. The beam track and the decay track were constrained to meet at a vertex. For the successful fits, the position of the vertex was required to be in a fiducial volume extending from the beam defining magnet to 5 m upstream of the drift chambers.

The largest backgrounds in this experiment were interactions and $\Sigma^+ \rightarrow p\pi^0$ decays in the PWCs. The PWC track fit confidence level cut suppresses interactions and decays in the PWCs and the fiducial volume cut eliminates most interactions in the drift chambers. The resolution on the vertex position in z was about 1 meter and, therefore, not adequate to distinguish reliably between interactions in the PWC region and the bulk of the good events which occur just downstream of the PWCs.

After imposing the above requirements, there remained a large number of events where the decay track had small transverse momentum relative to the beam track. These events could be caused by Σ^+ decays in the PWC region or quasi-elastic interactions. These events were eliminated by requiring the decay track to have ≥ 30 MeV/c transverse to the beam track. Information from the lead glass was not used except in the

trigger. Figure 2 shows the Σ^+ mass calculated assuming the decay mode $\Sigma^+ \rightarrow p\pi^0$. The background under the clear Σ^+ peak is less than 10%. We are able to see a signal from $K^+ \rightarrow \pi^+\pi^0$; this decay constitutes less than 1% of the events.

To analyze the decay angular distributions, each event was kinematically fit to the hypothesis $\Sigma^+ \rightarrow p\pi^0$ and the decay angles θ and ϕ were calculated where

$$\theta = \cos^{-1}(p_z/p); \quad \phi = \tan^{-1}(p_y/p_x) \quad (3)$$

and $\vec{p} = (p_x, p_y, p_z)$ is the proton momentum in the Σ^+ rest frame. Instead of the 30 MeV/c transverse momentum cut on the raw data, a somewhat more stringent cut, $|\cos \theta| < 0.94$, was imposed.

The polarization was obtained from the decay angular distribution for each targeting angle. Data from targeting angles ± 2.5 , ± 3.2 , ± 5.0 , and ± 7.0 mrad were available. The data were binned in 100 bins (10 in $\cos \theta$ x 10 in ϕ) for each of the eight targeting angles. The distribution is assumed to be

$$\frac{dN}{d\cos\theta \cdot d\phi} = \frac{N}{4\pi} \cdot A(\theta, \phi) \cdot (1 + \alpha \cdot \vec{P} \cdot \hat{n}) \quad (4)$$

where $A(\theta, \phi)$ is the acceptance, \hat{n} is a unit vector along the decay proton direction and \vec{P} is the polarization with components given by:

$$P_x = P \cdot \sin\psi \cdot \cos\xi \quad (5A)$$

$$P_y = P \cdot \cos\psi \quad (5B)$$

$$P_z = P \cdot \sin\psi \cdot \sin\xi. \quad (5C)$$

The analyzing power⁶ ($\alpha = -0.979 \pm 0.016$) is very favorable for analysis of the polarization in the $\Sigma^+ \rightarrow p\pi^0$ decay mode. When the targeting angle is reversed from positive to negative, the x and z components of the polarization change sign. If P_y is zero (as is expected from parity conservation) or changes sign when the targeting angle is reversed, then $A(\theta, \phi)$ can be found from any symmetric pair of targeting angles. On the other hand, if $A(\theta, \phi)$ is independent of ϕ , P_y can be found from the data. The former assumption is a slightly better fit to the data, although both assumptions yield the same result for the magnetic moment. It is important to note that, while $A(\theta, \phi)$ is intended to describe the acceptance of the apparatus, it also corrects for backgrounds and biases to order αP . This is a crucial point, since the experiment effectively measures the asymmetry by comparing positive and negative targeting angles, thereby benefiting from the cancellation of biases that would be present if either targeting angle was taken alone.

The data were fit using a maximum likelihood method with 112 parameters. Of these, 100 gave the values $A(\theta, \phi)$ for the 100 data bins, 7 were for normalization, 4 of these gave the absolute value of the polarization at the 4 targeting angles and 1 parameter (ξ) gave the rotation angle. The fit with a $\chi^2=740$ for 695 degrees of freedom gave $\xi = 1.01 \pm 0.05$ rad.

Several checks were made on this result. Different values of ξ were fit for each targeting angle. They were each consistent (within 1σ) of the average value given above. A more stringent event selection requiring a 1% confidence level for the $\Sigma^+ \rightarrow p\pi^0$ hypothesis, which should substantially reject background events, changes ξ by 0.03 rad.

The magnetic field calibration was accomplished with beam track data and $\Sigma^+ \rightarrow n\pi^+$ triggers. Beam track triggers (which consist mostly of non-interacting protons) were used to adjust the relative normalizations of the upstream and downstream spectrometer magnets. The adjustments were made on each run and had an rms spread of 0.3%, which is a measure of the systematic error in the calibration (due, e.g., to small drifts in chamber positions). The overall normalization of the spectrometer was found by requiring the Σ^+ mass reconstructed from the $n\pi^+$ decay mode to be equal to the accepted value⁶ of 1.1894 GeV. The mass normalization does not vary from run to run beyond about 0.2%, which is our ability to determine it. With this calibration the average momentum of particles exiting the channel is known to about 0.4%. From the construction of the channel, the bend angle of the central trajectory is 20.59 mrad. Since the beam particles do not uniformly populate the channel, the difference between the direction of the average beam particle and the center of the channel is only known to 80 μ rad. This latter error is dominant. We find that the $\langle \eta \rangle$ for a Σ^+ on the central trajectory of the channel is 175.8 ± 1.5 . Other checks of possible systematic biases included verification that the final sample of Σ^+ had a lifetime consistent with the accepted value⁶. The data

analysis codes were checked by generating $\Sigma^+ \rightarrow p\pi^0$ decays using Monte Carlo techniques and the measured experimental resolutions and requiring that the analyses reproduced the input Σ^+ polarization in direction and magnitude.

The same data sample was analyzed independently using directly measured quantities and not subjecting them to the possible biases of geometrical and kinematical fitting procedures. In this analysis, the three polarization components were analyzed separately with $\hat{n}=(\hat{x},\hat{y},\hat{z})$ and integrating over ϕ giving polarization and acceptance functions in terms of the three direction cosines, $\cos \theta_i$, with $i=1,2,3$. Using the ratio ($R_i(\cos \theta_i)$) of distributions from runs with equal and opposite targeting angles, both the acceptance functions, $A_i(\cos \theta_i)$, and the individual distribution in $\cos \theta_i$ are extracted. Figure 3 shows these distributions for the ± 5 mrad data. The plots of A_i illustrate the uniformity of our acceptance and the fall off at the edges of the $\cos \theta_i$ plots indicate the angular resolution in these center of mass quantities. The results obtained with this analysis are fully consistent with the earlier described analysis.

In Fig. 4a is shown the polarization vector of the Σ^+ at each of the four targeting angles. The polarization vs p_t is shown in Fig. 4b, along with the data⁷ of Wilkinson, et al. There is qualitative agreement between the two data samples; however, only the data at $p_t=1.0$ GeV/c were taken at the same value⁸ of Feynman x . The polarization is in the direction of the vector product of the incident proton and produced Σ^+ momentum. This is opposite to the polarization direction of inclusively produced lambdas.⁹

In order to obtain agreement between the spin rotation angle and the previously measured value⁶ of the magnetic moment $\mu_{\Sigma^+} = 2.30 \pm 0.14 \mu_N$, we must assume that the full rotation angle is $\xi + 2\pi$ or $\xi = 7.29 \pm 0.05$ rad. Applying (1) and (2) with the values of ξ , η and θ_B given above we find $\mu_{\Sigma^+} = 2.38 \pm 0.02 \mu_N$, where the error includes the statistical (0.014) and the systematic (0.014) contributions.

The simple SU(6) static quark model³ predicts a value for the Σ^+ magnetic moment of $2.67 \mu_N$. The disagreement of $0.29 \mu_N$ between this prediction and the measurement reported here is an order of magnitude larger than either the measurement uncertainty or the uncertainty due to experimental errors in the input parameters of the theory. Recent theoretical work⁴ has attempted to improve the agreement of this type of model with the measured baryon magnetic moments. At present no model adequately fits all the measurements.

We are grateful to the staff of Fermilab, particularly the Proton, Physics, and the Computing Departments for their assistance in completing this experiment. This work was supported in part by the U.S. Department of Energy under Contract Numbers DE-AC-02-76-CHO-3000 and DE-AC-02-76-ERO-3075.

REFERENCES

- a) Present address: Institute of Physics, Warsaw University, Warsaw, Poland.
- b) Present address: Department of High Energy Physics, University of Helsinki, Helsinki.
1. A cursory search located 72 articles published on this subject since 1978. Six of these articles reported new experimental results.
 2. The first such experiment was reported by L. Schachinger, et al., Phys. Rev. Lett. 41, 1348 (1978).
 3. A. De Rujula, H. Georgi, S.L. Glashow, Phys. Rev. D12, 147 (1975).
 4. Y. Tomozawa, Phys. Rev. D25, 795 (1982); A. Bohm and R.B. Teese, Phys. Rev. D26, 1103 (1982); J. Franklin, Phys. Rev. D20, 1742 (1979); H. Lipkin, Phys. Rev. D24, 1437 (1981), and references therein.
 5. C. Bernard, et al., Phys. Rev. Lett. 49, 1076 (1982); G. Martinelli, et al., Phys. Lett. 116B, 434 (1982).
 6. Particle Data Group, Phys. Lett. 111B, (1982).
 7. C. Wilkinson, et al., Phys. Rev. Lett. 41, 607 (1978).
 8. Here Feynman x is approximated by the Σ^+ secondary momentum divided by the incident proton momentum: $x = 212 \text{ (GeV/c)} / 400 \text{ (GeV/c)} = 0.53$.
 9. G. Bunce, et al., Phys. Rev. Lett. 36, 1113 (1976).

FIGURE CAPTIONS

- Figure 1 Plan view of the apparatus; scale is in meters.
- Figure 2 The reconstructed Σ^+ mass distribution. The full width at half maximum is $20 \text{ MeV}/c^2$.
- Figure 3 Acceptance functions $A_i(\cos\theta_i)$ and $\alpha P_i \cos\theta_i = (1-R_i)/(1+R_i)$ for the directions $i=x, y,$ and z as described in the text.
- Figure 4 (a) Σ^+ polarization components. The points are labeled by the corresponding vertical targeting angles in mrad. The angle ξ is the average precession angle modulo 2π . (b) The magnitude of the Σ^+ production polarization versus p_t , the Σ^+ transverse momentum. All data from this experiment are at a Feynman x of 0.53. The data of Ref. 7 have $x = p_t/2.0(\text{GeV}/c)$.

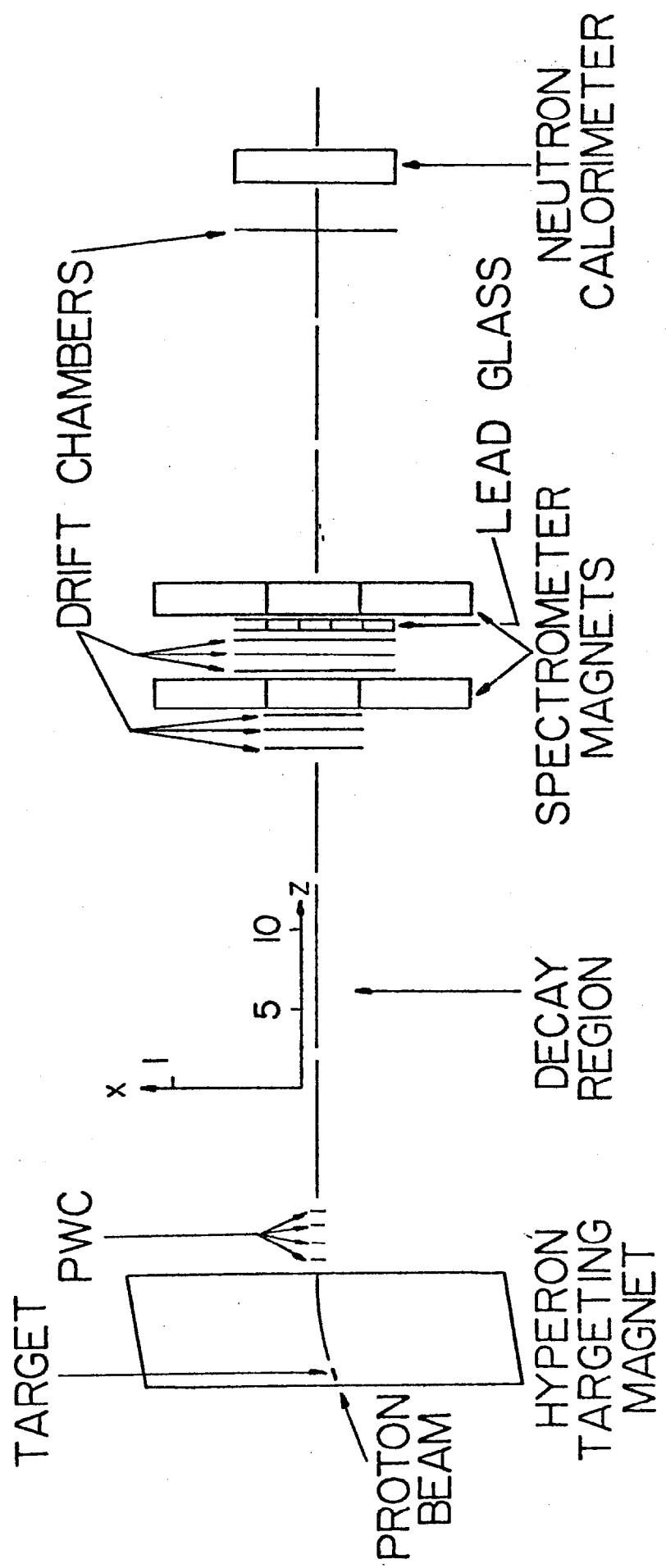
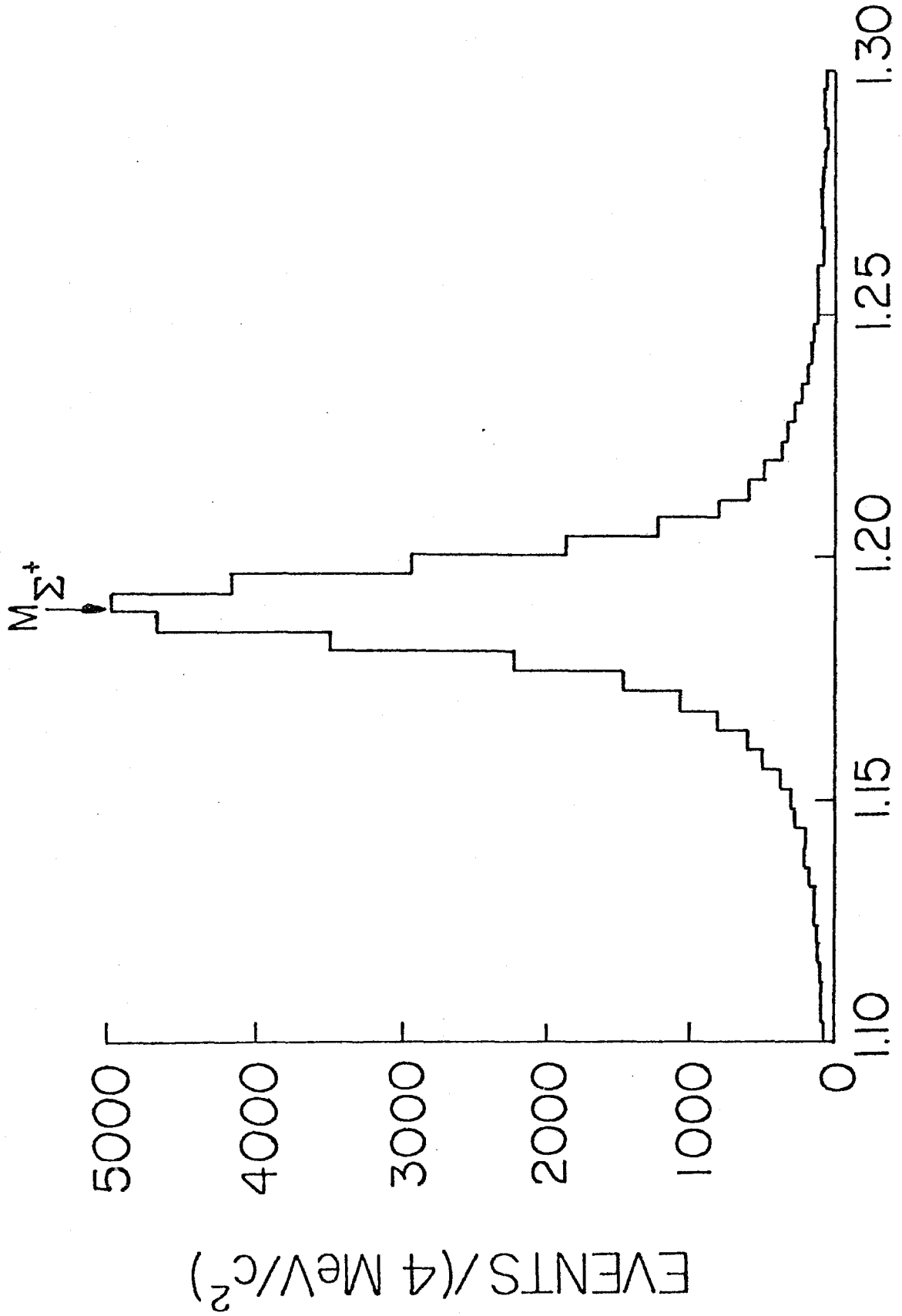


Fig. 1



$p\pi^0$ EFFECTIVE MASS(GeV/c²)

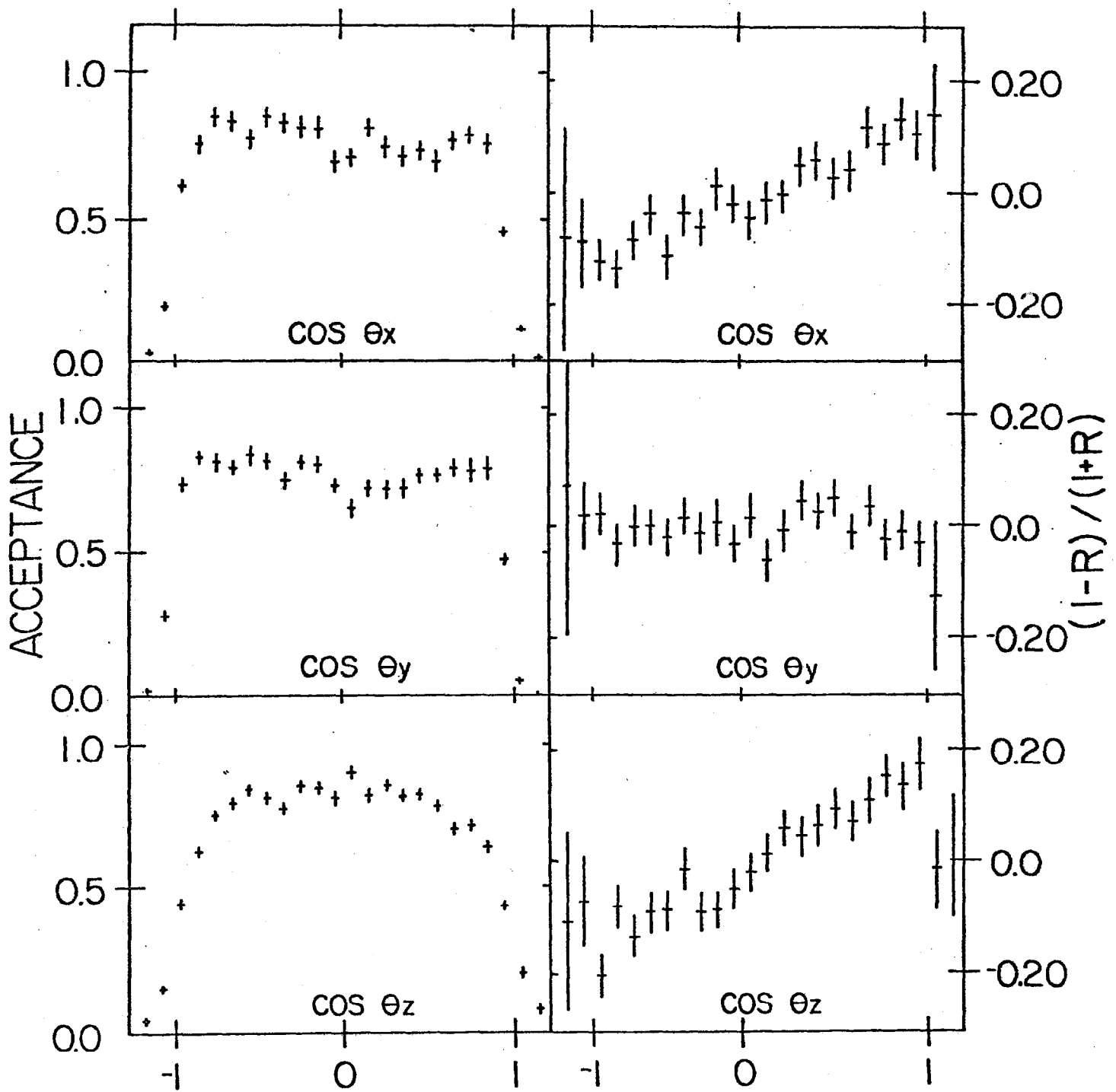


Fig. 3

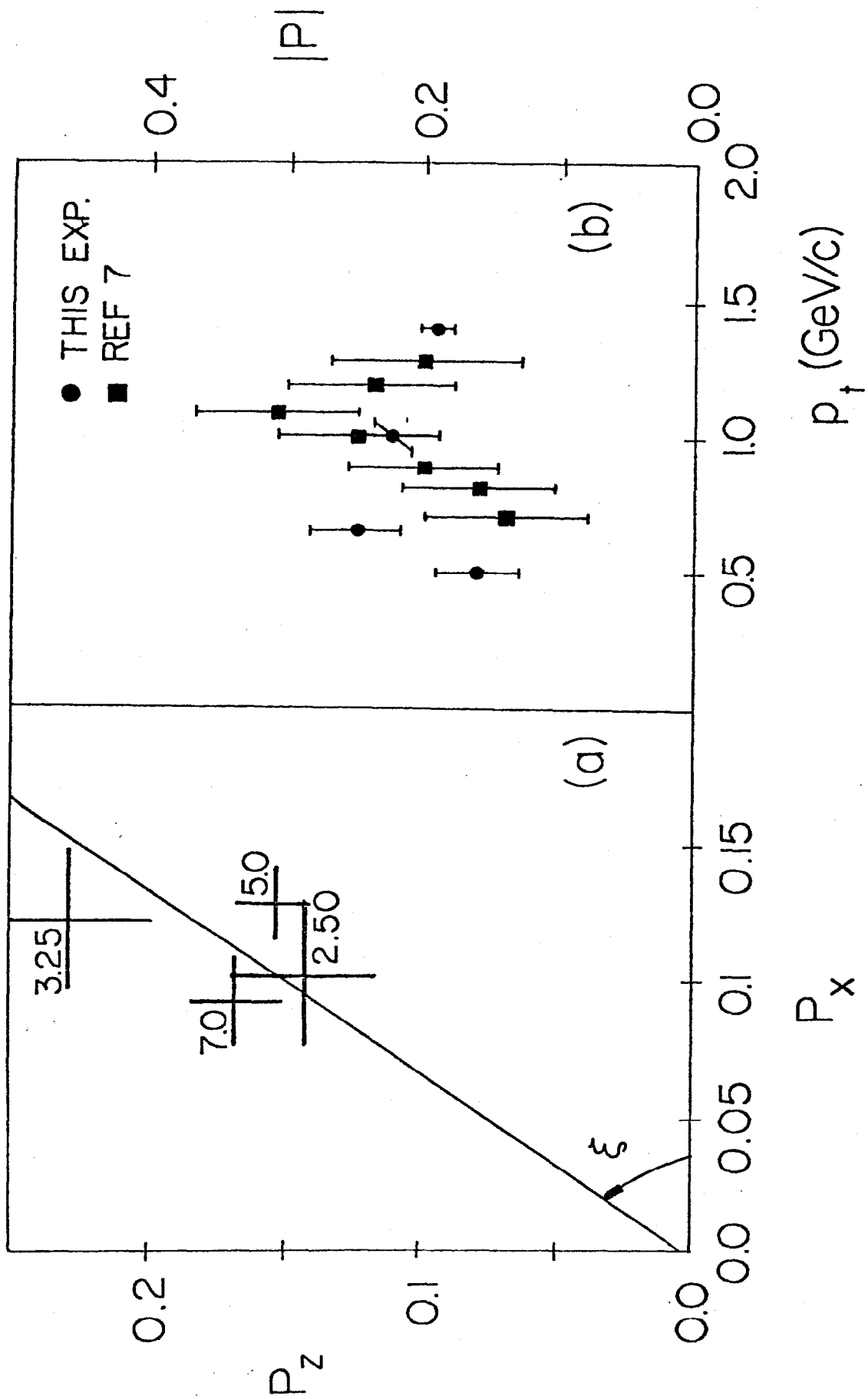


Fig. 4